

LASER-SCANNING AND 1D WAVELET TRANSFORMS FOR ARTIFICIAL DRAINAGE NETWORKS DETECTION IN MEDITERRANEAN RURAL LANDSCAPES

J.S. Bailly^{a*}, C. Millier^b, D. Saïdouni^a, P. Lagacherie^c

^aUMR 3S, ENGREF-Cemagref, 500 rue Jean-François Breton, 34093 Montpellier Cedex 5, France, (bailly-saidouni)@teledetection.fr

^bENGREF, 19 avenue du Maine 75732 Paris Cedex 15, France, millier@engref.fr

^cUMR LISAH, 2 place Vialla, INRA, 34060 Montpellier Cedex, France, lagacherie@ensam.inra.fr

KEY WORDS: LiDAR, Wavelets, Drainage Network, Ditches, Detection, Classification

ABSTRACT:

Artificial drainage networks such as ditches networks are landscape elements that control many hydrological transfers. To introduce these elements in hydrological models, we need to develop methods that allow their representation in space. We aimed here to assess the utilities of LiDAR data in the detecting and characterizing of ditches in Mediterranean cultivated rural landscapes. To perform the detection, we combined jointly laser-scanning and parcel boundaries data and developed a methodology based on: 1- estimation from last pulse laser points of terrain altimetric profiles that are perpendicular to parcel boundaries; 2- 1D wavelet transforms of the profiles; 3- a supervised classification of profiles with CART on the wavelet coefficients that are relevant for the size of the shapes we want to detect. The methodology we developed was applied in France on a typical basin of the Mediterranean vineyard landscapes. Compared to visual interpretation of the profiles, we obtained satisfactory detection rate. According to these results, high resolution laser-scanning data appears reliable for ditches detection but, due to vegetation and sampling resolution, misclassification on ditches typology is still important.

1 INTRODUCTION

Artificial drainage networks such as ditches, roads, are the features of cultivated landscapes that control many water flow related mass transfers: water, pollutants, sediments (Louchart et al. , 2001). The need to develop methods that allow the representation of these landscape elements in space and time, particularly for distributed hydrological models, has been often highlighted (Ambrose, 1999). To that end, the use of very high resolution remote sensing techniques appears relevant but has not been evaluated yet. In particular, high spatial definition laser-scanning supplies altimetric information, with partial discrimination between surface and terrain altimetry, at a scale that seems consistent with the sizes of artificial surface hydraulic network features (Gomes and Wicherson, 1999).

The present work aims to assess the utilities of laser-scanning in the detecting and the characterizing of ditches linear features in cultivated areas. As ditches are almost exclusively located on plot boundaries, we decided to focus on methods that analyze altimetric profiles which were automatically represented perpendicularly to plot boundaries. Consequently, our objective was to develop a methodology that classify 1D signals (the altimetric profiles) in a binary mode (ditches presence/absence) or in types of ditch for each plot boundaries location. For such shape analysis in

1D signals (Antoine et al., 1997), the utility of wavelet analysis has been proved for different applications: in medical studies (Sternickel, 2002), in financial time series analysis (Struzik, 2000), in LiDAR backscattering analysis (Quante et al., 2002) or LiDAR noise analysis (Fand and Huang, 2004) and in forest stand analysis from canopy LiDAR altimetric profiles (Ollier et al., 2003). Wavelets has the advantage to propose a multi-resolution analysis of a signal (Mallat, 1989). Thus, we may analyze the part of the noise-free signal that corresponds to the resolutions consistent with the studied objects and use classification models on wavelet coefficients at these resolutions. The methodology based on wavelets we developed was applied on the artificial drainage network of the Roujan basin, situated in the south of France. This area is cultivated and is typical of the Mediterranean vineyard landscapes. This paper is organized as follows. Section 2 presents discrete wavelet analysis illustrated on virtual altimetric profiles. In section 3, we describe briefly the data and their quality. The results of classification models based on wavelet coefficients for ditches detection are presented in section 4.

2 WAVELET ANALYSIS OF 1D SIGNALS

2.1 Wavelet Properties

Discrete wavelet transform (**DWT**) corresponds to a transform that decompose a discrete signal $z(t)$ into a set of basis functions that are obtained from a pair of orthogonal wavelet functions: ϕ , the father function and ψ , the mother function. The wavelets pair presented in figure 1 is the first orthogonal wavelet functions pair proposed by Haar (Haar, 1910) that present simple shapes, reliable to ditches shapes.

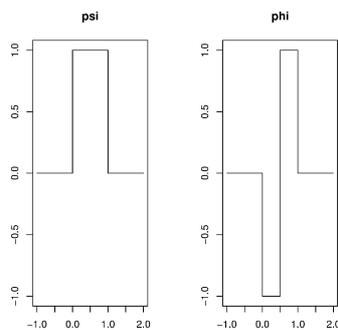


FIG. 1 – Haar wavelets pair

The wavelet approximation (wavelet transform) of the 1D signal $z(t)$ is given by :

$$z(t) \approx \sum_k S_{J,k} \phi_{J,k}(t) + \sum_{j=1}^{J-1} \sum_{k=0}^{n_j-1} d_{j,k} \psi_{j,k}(t) \quad (1)$$

In equation 1, j is called *resolution* or *scale parameter* going from J , the wider resolution, to 1, the finest resolution. k is a *translation parameter* going from 0 to $n_j - 1$, with n_j corresponding to the number of coefficients at resolution j .

$\int \phi(t)dt = 1$ so ϕ approximate the signal trend.
 $\int \psi(t)dt = 0$ so ψ is more traducing the signal details.
 The general principle of the wavelet transform is to approximate $z(t)$ with increasing resolutions through scaling and translations of ψ and ϕ functions. This generates $\phi_{J,k}(t)$ and $\psi_{j,k}(t)$ in equation 1. For dyadic resolutions, we obtain :

$$\phi_{J,k}(t) = 2^{-\frac{J}{2}} \phi\left(\frac{t - 2^J k}{2^J}\right) \quad (2)$$

and

$$\psi_{j,k}(t) = 2^{-\frac{j}{2}} \psi\left(\frac{t - 2^j k}{2^j}\right) \quad (3)$$

The coefficients $S_{J,k}, d_{J,k}, \dots, d_{1,k}$ are the wavelet transform coefficients. The detailed coefficients $d_{j,k}$ are approximatively given by the integrals

$$d_{j,k} \approx \int \psi_{j,k}(t) z(t) dt \text{ for } j = 1, \dots, J \quad (4)$$

The magnitude of the coefficients gives a measure of the contribution of the corresponding wavelet function to the approximating sum (Bruce and Gao, 1996): coefficients from different resolutions are straightforwardly comparable.

To better visualize how wavelet transform works, figure 2 shows on the top an example of a discrete signal $z(t)$ with 32 values and its transforms through 2 resolutions: from $r = 8 = 2^3$ (4 translations) to $r = 16 = 2^4 = 2^J$ (2 translations). The sub-figures situated on the figure 2 first column represent the values of the coefficients $S_{J,k}$ and $d_{j,k}$ coming from equation 4. On the second column, the scaled and translated wavelet functions $\phi_{J,k}(t)$ and $\psi_{j,k}(t)$ (Eq. 3, 2) are represented in different grey levels. On the third column, the part of the signal we want to approximate with functions of the second column is in black and in grey, we depicted the second column functions multiplied by wavelet coefficients in the first column. In the column on the right, we represented the residuals from previous approximation of the black line by the grey one. These residuals becomes the part of the signal to be approximate at the next finer resolution (next line on the figure). On this example $z(t)$ is almost totally captured by the wider resolution $r = 16$.

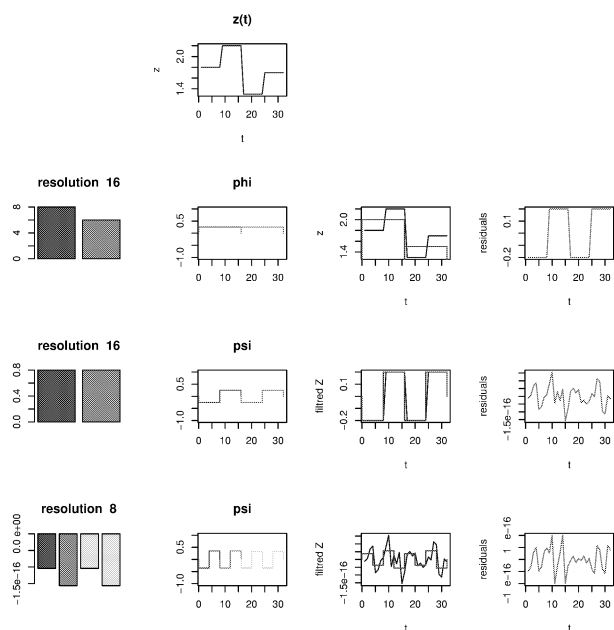


FIG. 2 – Example of $z(t)$ transform with Haar wavelets

2.2 Signals comparison with wavelet coefficients

Scalogram (Bruce and Gao, 1996) represents mother wavelet (detailed) coefficients on a *resolution, j* versus *time, k* plot : each coefficient is represented by the same area (high and narrow for the finest resolutions), filled

with coefficient value on a grey level look-up table. Coefficients at the same resolution are ordered on a scalogram line with order corresponding to translations coefficients k . On figure 3, 4 virtual altimetric profiles with depressions corresponding to ditches are represented. The scalograms of these 4 profiles illustrate how wavelet coefficients are traducing the presence and the type of depression and how detailed wavelet coefficients may be discriminant variables for ditches detection and characterization :

- a depression induces a succession of high negative then high positive values due to Haar ϕ shape, at a resolution corresponding to the width of the depression (see profiles 1 and 4),
- general shape of the profile is captured by the wider resolution ($r = 16$) and does not affect depression traduced by coefficients at smaller resolution (see profiles 1 and 2),
- the location of the positive/negative values in the scalogram is related to the location of the depression on the profile (see profiles 1 and 3).

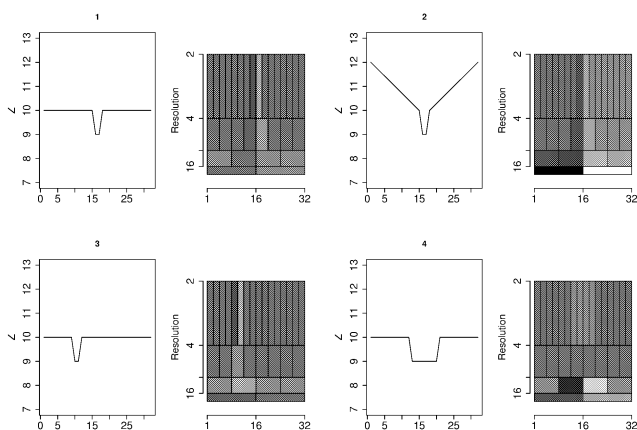


FIG. 3 – Virtual altimetric profiles and scalograms of detailed Haar wavelet coefficients on a grey look-up table from -2.5 (black) to 2.5 (white)

3 DATA

3.1 LiDAR acquisition

Data were acquired on a 2km^2 test area, part of the *Peyne* basin situated in the South of France. This area was selected while it's a representative area of the Languedoc vineyard landscape. This landscape is presenting many erosion, pollution and flooding problems (Lagacherie et al., 2004). It is containing complex and dense artificial drainage networks related to previous problems. These networks are mainly made of ditches. Ditches are presenting an high variability of sections, going from 0.06 to 5m^2 (with widths going from 0.3

to 2.5m), this affecting hydraulic capacities of the networks. Ditches are more or less maintained by farmers and some are highly covered by vegetation. A Geolas LiDAR mission with Toposys system was realized in June 2002 with helicopter over the test area. This mission provided multi-pulses scatter of 3D points with a mean of 10 spot measurements per m^2 , irregularly distributed in space.

3.2 Terrain altimetric profiles representation

We automatically represented altimetric profiles perpendicular to plot boundaries using jointly last pulse LiDAR 3D points and plot boundaries database on a GIS: 1- locations along plot boundaries were almost regularly selected with a 10 meters lag, then coordinates and azimuth of the boundary were attributed to each location; 2- LiDAR points were selected for each plot boundaries location within a 5 meters radius from the plot boundaries and with a thickness of 2 meters (figure 4-A). From this scatter of points projected on the 10 m profile length (figure 4-B), we estimated a regular 32 values profile using: 1 – first decile statistic when there were several measurements at a bin of the profile and, 2– linear interpolation when measurements were missing, 3 – then an open filter on the regular profile obtained previously with a structural element of about 1m (Soille, 1999) to remove residual vegetation, in particular vines (figure 4-B). The parameters of the process was optimized by comparison with ground truth topographic profiles (Saidouni, 2003).

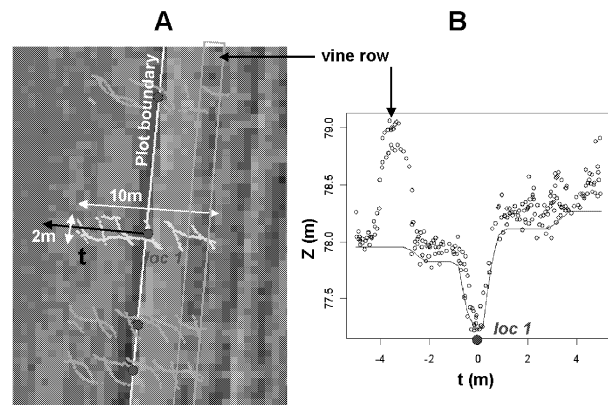


FIG. 4 – Example of altimetric terrain profile estimation perpendicular to a plot boundary at loc1 (location 1): Selection of LiDAR points for each plot boundary location plotted on an IRC 0.5 m resolution image for A and transformation of irregular scatter of topographic points (black points) to regular profile (line) for B

7018 altimetric profiles were such obtained on the 2 km^2 test area. For each profile, exhaustive ground survey

(Lagacherie et al., 2004) informed if it exists a ditch in its center, then the section of the ditch (width, depth). A visual classification of each profile where it exists a ditch was performed in 3 classes: with clear and apparent depression, without any depression and intermediary case. On these 2590 profiles, only 52% were presenting a clear depression. This prefigures the detection rate on ditches we may hope with the data.

4 RESULTS OF DITCHES DETECTION ON ALTIMETRIC PROFILES

Classification models on mother wavelet coefficients were performed using CART classification method (Breiman et al., 1984) with deviance as partitioning criterion. This classification method presents the advantage to not assume a specific distribution of classes in variables space. This method is too quite explicit to interpret the models. Resampling method on the 7018 profiles was used to asses the stability of classification models and results: for each classification, 500 profiles of each type were randomly selected then 70 % were randomly selected for model calibration, and the others 30% were used for cross-validation. For each classification, a CART model was calibrated on coefficients of resolution $r = 16,8,4$ as the example shown on figure 5 then good classification rate and confusion matrix were computed.

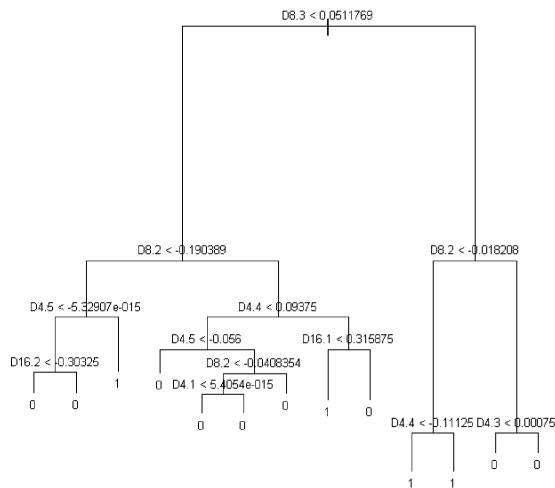


FIG. 5 – Example of CART model on wavelet coefficient for ditches presence-absence classification: D8.3 means resolution $r = 8$, $k = 3 - 1 = 2$ (third coefficient at this resolution)

On 100 classifications with resampling, we obtained:

- tree classification models that were mainly based

on central coefficients for resolutions $r = 8,4$ as seen on figure 5

- a mean of 82 % of good classification rate when calibrations and cross-validations were using only samples with ditches that presented visually a clear depression, with a well balanced confusion matrix between the two classes,
- a mean of 66 % of good classification rate when calibrations were using only samples with ditches that presented visually a clear depression and cross-validations were using all samples with ditches. But for that case, we observed an unbalanced confusion matrix between classes: 80 % of good classification for non ditches locations and 50 % for ditches locations. One of this model applied on all 7018 samples of the test area is presented in the left of the figure 6: locations classified with ditch are depicted in light grey. On the right image of figure 6, we can see in light grey the ditches locations coming from ground survey.



FIG. 6 – Comparison between classification of ditches presence (light grey) on the left and ground truth data on the right for each plot boundary location on the 2km² test area

5 DISCUSSION

If ditches locations along plot boundaries look poorly detected, this may be due to the data themselves (depression on altimetric profile) rather than the analysis method of the data when comparing to a visual interpretation of the data. This may be explained by the poor terrain altimetric information due to importance of vegetation masking ditches depression during data acquisition compared to laser power. This result of ditches detection should be balanced regarding

that 80 % of the plot boundaries locations without ditches, representing 67% of the studied locations on test area, are well classified. Looking at the spatial distribution of the classification results, well maintained ditches in openfields which are the main elements for drainage networks are the ones that are clearly detected. Whatever, these results shows than the automatization with wavelets for such shape characterization is highly suitable. We may easily imagine than the same approach may be reproduced with other types of data: LiDAR during winter season, radiometric profiles using very high resolution images.

For ditches characterization, tree models present leaves that seems to correspond to types of ditches (classes of width, depth) but some first results showed that misclassifications on types of ditches are still very high. This may due both to vegetation cover of the ditches that perturbs the shape in altimetric profile and to spatial resolution of LiDAR spot measurements that seems too large for precise discrimination between types of ditches.

These remote sensing results is just a first step to reach the final objective that is to map a probable artificial drainage network on plot boundaries space. To go further, these results could be used to condition the reconstruction of a set of probable artificial networks. To that end, remote sensing results on individual plot boundaries location could be aggregate -1- at plot boundary scale then -2- at whole basin scale to reconstruct drainage networks corresponding to oriented trees from the plot boundary lattice using topographic and topological rules.

Références

- Ambroise, B., 1999. *La dynamique du cycle de l'eau*. HGA
- Antoine, J., Barache, D., Cesar, R. and da Fontoura Costa, L., 1997. Shape characterization with the wavelet transform. *Signal processing*, 62, pp. 265–290.
- Breiman, L., Friedman, J., Olshen, R., and Stone, C., 1984. *Classification And Regression Tree*. Chapman.
- Bruce, A. and Gao, H., 1996, *Applied wavelet analysis with S-plus*. Springer.
- Fang, H.T. and Huang, D.S., 2004. Noise reduction in lidar signal based on discrete wavelet transform. *Optics communication*, 233, pp. 67-76.
- Gomes Perreira, L.M. Wicherson, R.J, 1999. Suitability of laser data for driving geogeographical information. A case study in the context of management of fluvial zone. *ISPRS Journal of Photogrammetry and Remote Sensing*, 542, pp. 105–114.
- Haar, A., 1910. Zur theorie der orthogonalen funktionen-systeme. *Math. Ann.*, 69, pp. 331–371.
- He, P., Fang, K. and Xu, C., 2003. The Classification Tree combined with SIR and its application to classification of Mass spectra. *Journal of data sciences*, 1, pp. 425–445.
- Lagacherie, P., Diot, O., Domange, N., Gouy, V., Floure, C., Kao, C., Moussa, R., Robbez-Masson, J. and Szleper, V., 2004. An indicator approach for describing the spatial variability of human-made stream network in regard with herbicide pollution in cultivated watershed, submitted to *Agriculture Ecosystems and Environment*.
- Louchart, X., Voltz, M., Andrieux, P. and Moussa, R., 2001, Herbicides runoff at field and watershed scales in a mediteranean vineyard area, *Journal of Environmental Quality*, 30(3), pp. 982-991.
- Mallat, S., 1989. A theory for multi-resolution signal decomposition : the wavelet representation. *IEEE Transactions on Pattern Analysis and Machine Intelligence*, 11 (7), pp. 674–693.
- Quante, M. Teschke, G., Zhariy, M., Maaß, P. and Sassen, K., 2002. Extraction and analysis of structural features in cloud radar and lidar data using wavelet based methods. *Proceedings of ERAD 2002*, pp.95-103.
- Ollier, S., Chessel, D., Couteron, P., Péliissier, R. and Thioulouse, J., 2003. Comparing and classifying one-dimensional spatial patterns: an application to laser altimeter profile. *Remote sensing of environment*, 85, pp. 453–462.
- Soille, P., 1999. *Morphological Image Analysis: Principles and Applications*. Springer-Verlag.
- Saidouni, D., 2003. Qualité et classification de données LiDAR multipulses pour l'extraction de réseaux d'écoulement en bassin rural aménagé. ULP Strasbourg, DESS ATS.
- Sternickel, K., 2002. Automatic pattern recognition in EGC time series. *Computer Methods and Programs in Biomedecine*, 68, pp. 109–115.
- Struzik, Z., 2000. Wavelet methods in financial time-series processing. *physica A*, 296, pp. 307–319.

Acknowledgements

This work was supported by the *PNTS*, the French National Program for Remote Sensing and by the *CNES* R&T program for flooding problems both for LiDAR data acquisition and general support.